The phase diagram of water at high pressures as obtained by computer simulations of the TIP4P/2005 model: the appearance of a plastic crystal phase

J. L. Aragones, M. M. Conde, E. G. Noya and C. Vega*

In this work the high pressure region of the phase diagram of water has been studied by computer simulation by using the TIP4P/2005 model of water. Free energy calculations were performed for ices VII and VIII and for the fluid phase to determine the melting curve of these ices. In addition, molecular dynamics simulations were performed at high temperatures (440 K) observing the spontaneous freezing of the liquid into a solid phase at pressures of about 80 000 bar. The analysis of the structure obtained lead to the conclusion that a plastic crystal phase was formed. In the plastic crystal phase the oxygen atoms were arranged forming a body center cubic structure, as in ice VII, but the water molecules were able to rotate almost freely. Free energy calculations were performed for this new phase, and it was found that for TIP4P/2005 this plastic crystal phase is thermodynamically stable with respect to ices VII and VIII for temperatures higher than about 400 K, although the precise value depends on the pressure. By using Gibbs–Duhem simulations, all coexistence lines were determined, and the phase diagram of the TIP4P/2005 model was obtained, including ices VIII and VII and the new plastic crystal phase. The TIP4P/2005 model is able to describe qualitatively the phase diagram of water. It would be of interest to study if such a plastic crystal phase does indeed exist for real water. The nearly spherical shape of water makes possible the formation of a plastic crystal phase at high temperatures. The formation of a plastic crystal phase at high temperatures (with a bcc arrangements of oxygen atoms) is fast from a kinetic point of view occurring in about 2 ns. This is in contrast to the nucleation of ice Ih which requires simulations of the order of hundreds of ns.

I. Introduction

The study of the phase diagram of water started its way with the pioneering work of Tammann[1,2] and Bridgman,[3–5] who obtained a number of different solid phases for water. The story has not ended yet since in the last decade new solid phases have been discovered, as it is the case of ice XII,[6] discovered in 1998 by Lobban, Finney and Kuhs and ices XIII and XIV discovered just two years ago by Salzmann et al.[7] In addition to the existence of new phases, water presents a number of interesting questions, as the possibility of a liquid–liquid transition,[8,9] the relation between the different amorphous phases,[10] the possibility of partial proton ordering[11] and the aspect of the phase diagram at high temperatures and pressures. Water is an important molecule since its liquid phase constitutes the "matrix of life".[12,13] Getting a molecular understanding of the behaviour of water[14] appears as an interesting and challenging goal. For this reason thousands of computer simulation studies have been reported since the pioneering work of Barker and Watts[15] and Rahman and Stillinger.[16] Most of the studies have focused on the liquid phase. The study of the solid phases have received less

Dpto. de Química Física, Facultad de Ciencias Químicas, Universidad Complutense, Madrid, 28040, Spain. E-mail: cvega@quim.ucm.es

attention. Morse and Rice[17] analysed the performance of early water models to describe the different solid phases of water. In the recent years we have analysed the performance of several popular models (SPC/E[18] and TIP4P[19]) to describe the solid phases of water and its phase diagram.[20–23] It was realized that TIP4P could be modified slightly to yield an overall better description of the water phase diagram. In this way we proposed two new models TIP4P/2005[24] and TIP4P/Ice,[25] the first describing correctly the maximum in density of water and the second reproducing the melting point temperature of ice Ih. After analysing the behaviour of these two models for other properties (diffusion coefficients, surface tension, vapour–liquid equilibria) it has been concluded that TIP4P/2005 provides a quite reasonable description of the properties of water. In fact it reproduces reasonably well the densities and relative energies of the water polymorphs,[26–28] the vapour–liquid equilibria,[29] the diffusion coefficient,[24] the surface tension[30] and the structure of the liquid and solid phase (as given by the radial distribution functions). In the original paper where TIP4P/2005 was proposed it was shown that it provides a reasonable description of the phase diagram of water[24] at low and moderate pressures where the polymorphs Ih, II, III, V and VI are thermodynamically stable. However, the high pressure and high temperature region was not considered. One of the goals of this paper is to determine the high

This journal is © the Owner Societies 2009

Phys. Chem. Chem. Phys., 2009, **11**, 543–555 | 543

temperature and the high pressure part of the phase diagram including the high pressure polymorphs, namely ices VII and VIII.

Another issue which motivated this research was the possibility of obtaining by computer simulation the nucleation of ice from liquid water. In principle, by cooling water at room pressure in a computer simulation, there is the possibility of nucleating ice Ih (or Ic). Svishchev and Kusalik[31] were able to nucleate ice from liquid water by using an external field. Attempts to obtain ice from water without an external field were unsuccessful until the seminal work of Matsumoto, Saito and Ohmine,[32] who in 2002 observed for the first time the nucleation of ice from liquid water after very long runs (hundreds of ns). After these first attempts several other authors have been able to nucleate ice from water. Vrbka and Jungwirth[33] nucleated ice from water in a very long run using a slab of liquid in contact with its vapour. Quigley and Rodger[34] nucleated ice by introducing bias in the simulations (via the metadynamics technique[35]). However, it is fair to say that nucleating ice Ih (or Ic) from liquid water in a computer simulation is rather difficult, and this can be achieved only either performing very long runs or introducing bias within the simulations. However, in a very recent experimental study following previous work,[36] Dolan et al.[37] showed that the formation of ice VII, from water occurs in a few nanoseconds when the temperature was around 400 K. In their work, Dolan et al.[37] suggested that such low nucleation time could be studied by computer simulation. We intend to address this issue in this paper.

In the present work we shall determine by using free energy calculations the high pressure region of the phase diagram of the TIP4P/2005 model. On the other hand we shall use this model to analyse if the nucleation of ice VII from the liquid does indeed occur in a few ns. As it will be shown the answer is positive, and besides, as a surprise a new solid phase is found for water. This new solid phase is a plastic crystal phase. It will be shown that for TIP4P/2005 this plastic crystal phase is thermodynamically stable with respect to ices VII and VIII in the region of high pressures and temperatures. The plastic crystal has also been found two months ago by Takii, Koga and Tanaka[38] for the TIP5P and TIP4P models of water. It would be of interest to determine if this plastic crystal phase does indeed exist for real water, especially taken into account that the interest in the high pressure phases of water is growing.[39,40] If so, that would be, ice XV (the precise value of the Roman numeral depends on the order ices are found experimentally).

II. Simulation details

In this work Monte Carlo simulations have been performed for ices VIII, VII and liquid water. The TIP4P/2005 model will be used. This is a rigid non-polarisable model, with a distribution of charges, similar to that of the TIP4P model. A Lennard-Jones (LJ) site is located on the oxygen atom, positive charges are located on the hydrogen atoms, and the negative charge is located in the H–O–H bisector. The parameters of the model are given in Table 1. The TIP4P/2005 model improves the description of water properties

significantly with respect to the original TIP4P model[41] and is becoming popular in computer simulations of water.[42–45] A critical comparison of the performance of the model with respect to other water models has been presented recently.[46]

Ice VIII is formed by two sub-lattices, which are interpenetrated but not interconnected.[47,48] In one of the sublattices all dipole moments of the water molecules are aligned along the negative direction of the vector **c** of the unit cell, whereas in the other sublattice all dipole moments are aligned along the positive direction of the **c** vector of the unit cell. Thus the net dipole moment of ice VIII is zero. Protons are ordered in ice VIII. Thus an initial configuration of ice VIII can be obtained easily from the neutron diffraction experimental data[49] (adjusting slightly the bond length and angles from the experimental values to those of the TIP4P/2005 model). Ice VII is formed by two ice Ic sublattices which are interpenetrated but not interconnected. Ice VII is a proton disordered phase.[48,50,51] The initial configuration of ice VII was obtained by generating first an ice Ic lattice, with no net dipole moment and satisfying the Bernal–Fowler rules.[52,53] The algorithm of Buch et al.[54] was used to obtain such a proton disordered configuration. A second ice Ic lattice was obtained in the same way. After these two independent ice Ic configurations were obtained, we generated the initial configuration of ice VII by putting together the two ice Ic sublattices, so that they are interpenetrated but not interconnected. Thus, the density of ice VII is of about twice the density of ice Ic.

The number of molecules used in the simulations were 600 (ice VIII), 432 (ice VII), 360 (ice VI) and for water we used either 432 or 360. In all cases the LJ potential was truncated at 8.5 Å. Standard long range corrections to the LJ part of the potential were added (i.e., $g(r) = 1$ beyond the cutoff).[55] Note that this simple prescription (i.e. assuming $g(r) = 1$ beyond the cutoff) might introduce an error in the estimate of the long range correction, especially in solid phases (where $g(r)$ is not one even at large distances). The impact that this might have on the coexistence points is not easy to assess, as the effect is different for different phases and at different densities. By analysing the internal energy of solid phases for different systems sizes we conclude that the use of the simple prescription $g(r) = 1$ to estimate the long range correction of the LJ part of the potential may introduce an error of about 1.5% in the determination of coexistence points, which is enough for the purposes of this work. The importance of an adequate treatment of the long range Coulombic forces when dealing with water simulations has been pointed out in recent studies.[56–58] In this work, the Ewald summation technique[59] has been employed for the calculation of the long range electrostatic forces. Isotropic NpT simulations were used for the liquid phase and for ice VII (which is of cubic symmetry) while anisotropic Monte Carlo simulations (Parrinello–Rahman like)[60,61] were used for ices VIII and VI (both tetragonal). A typical Monte Carlo run involves about 30 000 cycles of equilibration and 70 000 cycles to obtain averages (defining a cycle as a trial move per particle plus a trial volume change).

The free energy was computed at a certain thermodynamic state for the ices VIII, VII and for liquid water. Once obtained at a certain thermodynamic state the free energy can be

544 | *Phys. Chem. Chem. Phys.*, 2009, **11**, 543–555

This journal is © the Owner Societies 2009

Table 1 Parameters of the TIP4P/2005 model. The distance between the oxygen and hydrogen sites is d_{OH}. The angle formed by hydrogen, oxygen, and the other hydrogen atom is denoted by H–O–H. The LJ site is located on the oxygen with parameters σ and ε/K. The charge on the proton is q_H. The negative charge is placed in a point M at a distance d_{OM} from the oxygen along the H–O–H bisector

d_{OH} (Å)	H–O–H (°)	σ (Å)	ε/k_B (K)	q_H (e)	d_{OM} (Å)
0.9572	104.52	3.1589	93.2	0.5564	0.1546

computed for any other thermodynamic conditions by using thermodynamic integration. Initial coexistence points were located by imposing the condition of equal chemical potential, temperature and pressure between coexistence phases. In particular we located coexistence points between several phases along the 70 000 bar isobar, and along the 400 K isotherm. The free energy of the liquid is calculated by computing the free energy change along a reversible path in which the water molecules are transformed into Lennard-Jones spheres by switching off the charges. The free energy of the reference Lennard-Jones is taken from the work of Johnson *et al.*[62] The free energy of ices VIII and VII was obtained by using the Einstein crystal method,[63] or its slight variant recently proposed by us denoted as the Einstein molecule method.[64] In the case of ice VII, and due to the proton disorder, one must add at the end of the calculation the entropy contribution due to the degeneracy of the structure. Thus was estimated by Pauling[53] to be of about $S/(Nk_B) = \ln(3/2)$. Further details about the free energy calculations, both for the liquid phase, and for the solid phases of water can be found in our recent review paper about free energy calculations.[65]

Once an initial coexistence point has been determined the rest of the coexistence curve can be obtained by using Gibbs Duhem simulations.[66,67] Gibbs–Duhem simulations, first proposed by Kofke, allow to determine the coexistence line between two phases, provided that an initial coexistence point is known. Gibbs–Duhem is just a numerical integration (using simulation results to estimate the volume and enthalpy change between phases) of the Clapeyron equation. For the integration of the Clapeyron equation a fourth-order Runge–Kutta method algorithm is employed. Anisotropic scaling (Rahman Parrinello like) was used to simulate ices VIII and VI (both are tetragonal) and isotropic NpT simulations are used for the liquid and for the solid phases of cubic symmetry (ice VII and the plastic crystal solid). Rest of the details (size of the system, cutoff) were identical to that used in the NpT simulations.

In this work we have also performed Molecular Dynamic simulations to study the formation of solid phases from liquid water at high temperatures. The choice of Molecular Dynamics (instead of Monte Carlo) allows to determine the time required by the liquid to freeze so that a comparison with experiment is possible. The molecular dynamic simulations were performed with the program Gromacs.[68] In the simulations the temperature is with a Nose–Hoover thermostat[69,70] with a relaxation time of 2 ps. To keep the pressure constant, an isotropic Parrinello–Rahman barostat[71,72] was used. The relaxation time of the barostat was 2 ps. The time step used in the simulations was 1 fs. The typical length of the simulations was about 5 ns (five million time steps). The geometry of the water molecule is enforced using constraints. The LJ part of the potential was truncated at 8.5 Å and standard long range corrections were added. The real part of the Coulombic

potential was truncated at 8.5 Å. The Fourier part of the Ewald sums was evaluated by using the Particle Mesh Ewald (PME) method of Essmann *et al.*[73] The width of the mesh was 1 Å and we used a fourth other polynomial. As it can be seen the conditions of the Molecular Dynamic simulations were quite similar to those used in the Monte Carlo simulations.

III. Results

Let us start by presenting the results of Molecular Dynamics for the 440 K isotherm. This temperature is close to temperature where fast nucleation of ice was observed experimentally.[37] We used 432 molecules in these molecular dynamic simulations. The choice of this number of molecules was motivated by the fact that we were expecting the formation of ice VII at high pressures. This number of molecules (432) would correspond to 216 unit cells ($6 \times 6 \times 6$) of ice VII. We started our simulations at low pressures (*i.e.* about 10 000 bar) where the system is in the liquid phase, and increased the pressure in consecutive runs. The configuration of a run was used as the initial configuration of the next run. When the pressure was 80 000 bar we observed the spontaneous formation of a solid phase within a few ns. We repeated the runs several times (using different initial configurations) and the formation of the solid phase in less than 5 ns was observed in almost all the cases. Thus the nucleation of a solid phase under these thermodynamic conditions can be reproduced easily. In Fig. 1 the evolution of the density with time at 440 K and 80 000 bar is plotted for several independent runs (we performed five independent runs). The nucleation of ice is a
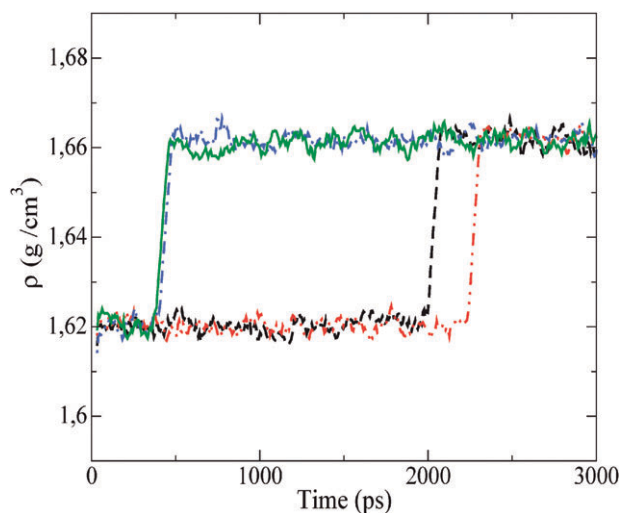

Fig. 1 MD trajectories for four different initial configurations obtained with Gromacs at 440 K and 80 000 bar. The formation a plastic crystal phase is indicated by the jump in the density (for two of the runs freezing occurs at quite similar times).

stochastic event so that each run freezes in a somewhat different time. However, it is clear that the formation of a solid phase occurs in about 1.5 ns for the TIP4P/2005 model in this thermodynamic state (although for one of the five runs performed no freezing was observed after 5 ns). Since the package Gromacs allows one to visualise the trajectories, it was simple to identify the structure of the solid. The oxygen atoms of the water molecules formed a body centred cubic structure. The surprise was that the molecules of water were rotating rather wildly in the solid phase. Thus the system jumped from the liquid phase into a plastic crystal phase. Notice that ices VIII and VII are not plastic crystal phases, so that the phase obtained spontaneously is a new type of solid. For small system sizes ($N = 128$ and $N = 432$) and NpT simulations the crystal formed tends to be commensurate with the simulation box. However, for larger system sizes or NVT simulations we found more often that the crystal grows in some direction that was not compatible with the simulation box, so that complete crystallisation could not be achieved. In summary, we have observed that the TIP4P/2005 model freezes spontaneously in about 1.5 ns (in average) into a plastic crystal phase at 440 K. The formation of a plastic crystal, by heating ice VII at constant pressure has also been reported two months ago by Takii, Koga and Tanaka[38] for the TIP5P and TIP4P models. The plastic crystal phase obtained in this work from the liquid is identical to that described by Takii, Koga and Tanaka.[38] Sometimes when cooling/compressing liquids, the obtained solid phase is not the most stable from a thermodynamic point of view, but the more favourable from a kinetic point of view. Thus the thermodynamic stability of the plastic crystal phase with respect to ices VIII and VII should be determined.

After observing the formation of the plastic crystal phase we analysed in detail the mechanical stability of ices VII and VIII when heated along the 70 000 bar isobar. Starting at low temperatures, the temperature was increased (in jumps of 10–20 K). For each temperature the length of the run was of about 100 000 cycles. The configuration of each simulation was taken as the initial configuration of the next run. For ice VII we observed a jump in the internal energy and density starting at a temperature of about 380 K and ending at a temperature of about 390 K. Visualisation of several snapshots revealed that the phase obtained at 390 K was a plastic crystal phase. The density, radial distribution functions and internal energy were identical to those of the plastic crystal phase obtained from the freezing of the liquid (when compared at the same thermodynamic conditions). This is illustrated for the radial distribution functions in Fig. 2. After a long equilibration at 400 K and 70 000 bar of the plastic crystal phase obtained by heating ice VII, we proceed to cool the system along the isobar to see if the system was able to return to the original state. The plastic crystal phase was mechanically stable up to 360 K, and at a temperature of about 350 K, the density and internal energy undergo a jump. The result of this heating–cooling cycle is plotted in Fig. 3. The presence of a hysteresis loop indicates clearly the existence of a first order phase transition between ice VII and the plastic crystal phase. In fact the phase obtained by cooling the plastic crystal phase is ice VII. In Fig. 4 the radial distribution functions
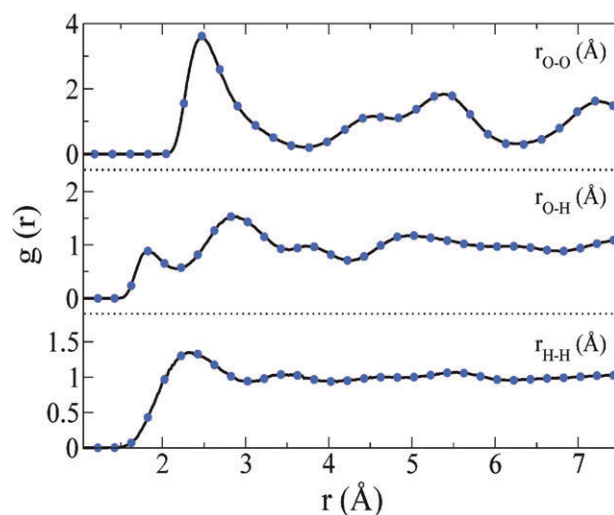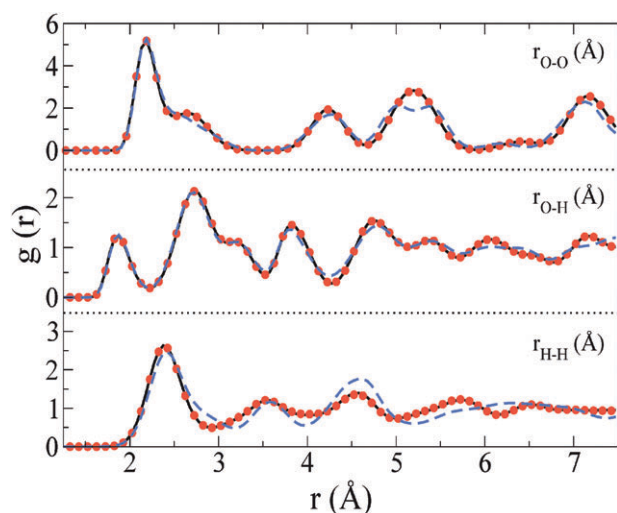

Fig. 2 Oxygen–oxygen, oxygen–hydrogen and hydrogen–hydrogen radial distribution functions at $T = 440$ K and $p = 80\,000$ bar for the bcc plastic crystal as obtained by isothermal compression of the liquid state (solid line) and by isobaric heating of ice VII (filled circles).
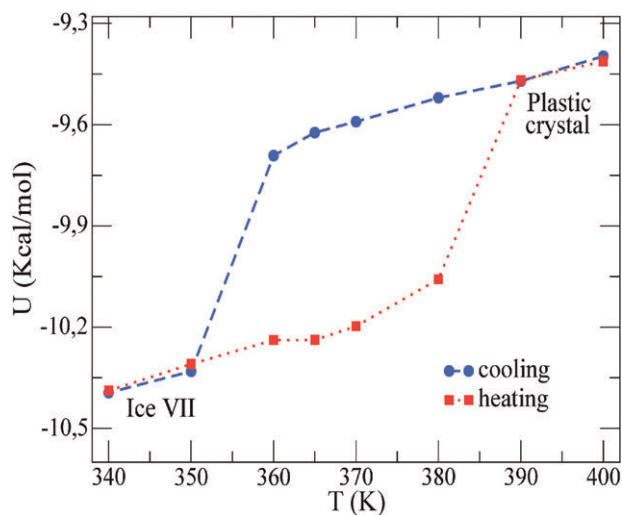
Fig. 3 Hysteresis loop obtained by heating ice VII to obtain the plastic crystal phase (dotted line) and by cooling the plastic crystal phase to recover ice VII (dashed line). Results were obtained along the 70 000 bar isobar. The residual part of the internal energy is plotted as a function of the temperature.

(O–O, H–H and O–H) of ice VII and of the phase obtained by cooling the plastic crystal phase are shown. As it can be seen they are nearly identical (and the same is true for other thermodynamic properties as density and internal energy) providing further evidence of the fact that the solid phase obtained by cooling the plastic crystal is ice VII. By analysing the average positions of the water molecules in the phase obtained from the cooling of the plastic crystal phase, we found that the solid was formed by two sublattices which are interpenetrated but not interconnected as in ice VII. In each of the sublattices each molecule was forming four hydrogen bonds (in two acting as donor and in two acting as acceptor). Therefore, the phase obtained by cooling the plastic crystal phase was indeed ice VII. We have repeated this

Fig. 4 Oxygen–oxygen, oxygen–hydrogen and hydrogen–hydrogen radial distribution functions for ice VII (solid line), for ice VII obtained from the cooling of the plastic crystal phase (filled circles) and for ice VIII (dashed–dotted line). The radial distribution functions were obtained at 300 K and 70 000 bar.

heating–cooling cycle for the ice VII-plastic crystal transition at several pressures (70 000 bar, 65 000 bar and 60 000 bar). In Table 2 the temperatures at which the ice VII to plastic crystal and plastic crystal to ice VII transitions occur are presented. From the results of Table 2 it is obvious that the ice VII to plastic crystal thermodynamic phase transition (where the chemical potential of both phases become identical) must be between 350 K and 390 K when the pressure is of 70 000 bar, between 340 K and 380 K when the pressure is 65 000 bar and between 310 K and 360 K when the pressure is of 60 000 bar.

Obviously only free energy calculations can determine the precise location of the coexistence point, which must be located between the two temperatures which bracket the hysteresis loop.

We also analysed the mechanical stability of ice VIII when heated along these three isobars. It was found that ice VIII was mechanically stable up to 390 K for the $p = 70\,000$ bar isobar, up to 390 K for the $p = 65\,000$ bar isobar and up to 380 K for the $p = 60\,000$ bar isobar. At higher temperatures ice VIII also becomes a plastic crystal phase. Thus ice VIII becomes mechanically unstable (transforming into a plastic crystal phase) at temperatures similar to those found for ice VII. The mechanical stability limit of ice VIII (where it transforms into a plastic crystal phase) seems to be about 10 K higher than that of ice VII. We did not observe any spontaneous transformation of ice VIII into ice VII when heated. This is not to say that this transition does not exist from a

thermodynamic point of view (in fact it will be shown later that this transition indeed exists) but rather that the system is not able to overcome the free energy nucleation barrier separating ice VIII from ice VII within the length of our simulations. In any case for pressures below 70 000 bar it is not possible to have neither ice VIII nor ice VII as mechanically stable phases for temperatures above 390 K. This provides further evidence that the plastic crystal phase obtained spontaneously from the liquid at 440 K must indeed be thermodynamically stable at least at high temperatures. In any case, the definite proof of that will be provided by the free energy calculations. In Fig. 4 the radial distribution functions of ice VIII are compared to those of ice VII at 300 K and 70 000 bar. They are clearly different showing that both solids are mechanically stable (and clearly distinguishable) under these thermodynamic conditions.

Let us now present the structural properties for the plastic crystal phase. In Fig. 5, the radial distribution functions for the plastic crystal phase at 400 K and 70 000 bar are compared to those of ice VII at 300 K and 70 000 bar for the O–O, O–H and H–H correlation functions. As it can be seen from the oxygen–oxygen correlation function, the peaks of the O–O distribution in the plastic crystal phase correspond to those of ice VII, although the higher temperature and lower density of the plastic crystal solid provokes peaks with a more diffuse character. Changes in the gO–H distribution function are significant, but the most important change occurs in the gH–H correlation function. It has a liquid like aspect in the plastic crystal solid whereas its long range order is clearly visible in ice VII. Thus the gH–H distribution function is quite useful to identify the existence of a plastic crystal phase.

We have also determined the probability distribution of the polar angles (θ and ϕ of the OH bonds). The x axis is located on the **a** vector of the unit cell, the y axis is located on the **b** vector of the unit cell, and the z axis is located along the
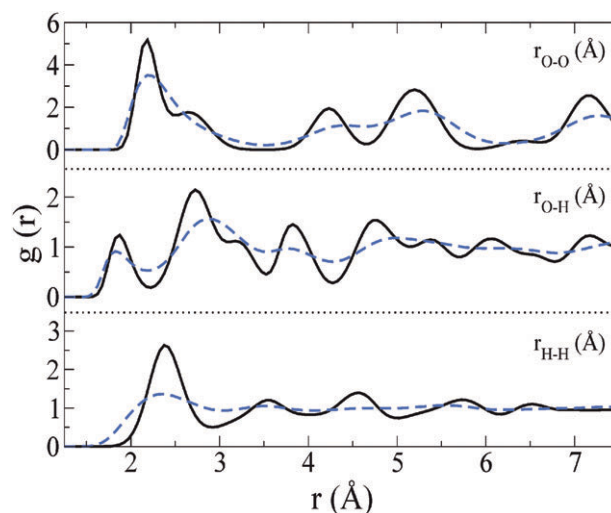
Table 2 Stability limits of ice VII when heated and of the plastic crystal phase when cooled as obtained from NpT simulations at three different pressures

p/bar	Ice VII-plastic crystal (*heating*)	Plastic crystal-ice VII (*cooling*)
70 000	390	350
65 000	380	340
60 000	360	310

Fig. 5 Oxygen–oxygen, oxygen–hydrogen and hydrogen–hydrogen radial distribution functions for ice VII at 300 K and 70 000 bar (solid line) and for the plastic crystal phase at 400 K and 70 000 bar (dashed–dotted line).
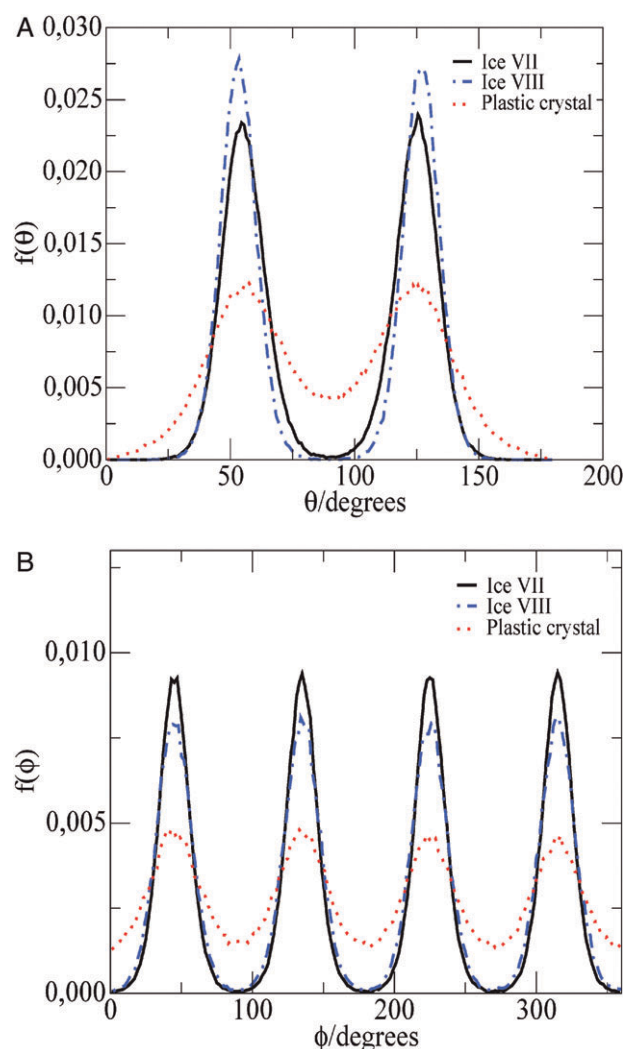
This journal is © the Owner Societies 2009

Phys. Chem. Chem. Phys., 2009, **11**, 543–555 | **547**

c vector of the unit cell. The distribution function $f(\theta)$ is defined as:

$$f(\theta) = \frac{N(\theta)}{2N\Delta\theta} \quad (1)$$

where $N(\theta)$ denotes the number of OH bonds with polar angle between θ and $\theta + \Delta\theta$ and $2N$ is the number of OH bonds (*i.e.* twice the number of molecules N). The distribution function $f(\phi)$ is defined as:

$$f(\phi) = \frac{N(\phi)}{2N\Delta\phi} \quad (2)$$

In Fig. 6 the functions $f(\theta)$ and $f(\phi)$ are presented for ices VIII and VII at 300 K and 70 000 bar. As it can be seen the peaks of $f(\theta)$ are located at 54.74 and (180–54.74) where 54.74 is the angle in ice VII between one of the diagonals of the cube and a line connecting the center of two opposite faces. The four

peaks in $f(\phi)$ are separated by 90 degrees as it should be. In Fig. 6 the functions $f(\theta)$ and $f(\phi)$ are also presented for the plastic crystal phase at 400 K and 70 000 bar. As it can be seen both distributions present less structure than the one of ices VII and VIII. It is also clear that even in the plastic crystal phase the OH vectors prefer to point out to the contiguous oxygen atoms. Therefore the angular distribution is not uniform even in the plastic crystal phase (*i.e.* the OH vector does not distribute uniformly on the surface of a sphere). The molecules, although able to rotate prefer to point the OH vectors towards any of the 8 O atoms forming the first coordination layer. However, we checked that as the temperature increases the $f(\theta)$ and $f(\phi)$ distributions become somewhat more uniform. In summary the molecules rotate almost freely in the plastic crystal phase, but the OH vectors prefer to point out to the contiguous oxygen atoms. An additional interesting comment is that for ices VIII and VII at 300 K and 70 000 bar and for the length of the simulations performed in this work, a certain individual molecule presents a value of θ and ϕ (except for a little bit of thermal vibration). However for the plastic crystal phase each individual molecule jumps quite often from one of the peaks of the distribution to another peak. These flipping or jumping moves occur quite often for each molecule within the length of the simulation runs considered here (at 400 K in average each flipping requires about 8000 Monte Carlo cycles). The ice VIII to ice VII transition represents the change from proton order to proton disorder within the two sub lattices of the solid, whereas the ice VII to plastic crystal phase transition represents the disappearance of the two sublattices.

Let us now change to the determination of coexistence points. We have determined the free energy for ices VIII, VII and for the plastic crystal phase (Table 3). The free energy calculation was performed for ice VIII at 300 K and for a density which corresponds to that of the system at 70 000 bar. The free energy of ice VII was computed at 300 K and for a density which corresponds to that of 70 000 bar. Finally the free energy of the plastic crystal phase was computed at 400 K and for a density which corresponds to that of the system at 70 000 bar. Details about the free energy calculations in water solid phases have been provided elsewhere.[65] Let us just mention the procedure used to compute the free energy of the plastic crystal phase as it differs from that used for the rest of solid phases of water. Firstly translational springs connecting the oxygen atoms to the lattice positions of the bcc structure were switched on (in the plastic crystal phase the oxygens form a bcc solid). After that, and while keeping the translational springs, the charges of the system were switched off ending with a system of LJ atoms connected by springs to a bcc solid structure. Free energies changes can be computed easily along this path in which the Hamiltonian of the system is changed. Notice that no phase transition occurs along the integration since the system is in a plastic crystal phase along the entire integration path. Finally the free energy difference between a LJ particle connected with translational springs to a bcc lattice, and an ideal Einstein crystal (with springs connecting to the bcc lattice but without intermolecular interactions) is computed by a perturbative approach. This integration path is inspired by a recent article by Lindberg

Fig. 6 (a) $f(\theta)$ as a function of θ angle for ices VII (solid line) and VIII (dashed–dotted line) at 300 K and 70 000 bar and for the plastic crystal phase (dotted line) at 400 K and 70 000 bar. (b) $f(\phi)$ as a function of ϕ angle for ices VII (solid line) and VIII (dashed–dotted line) at 300 K and 70 000 bar and for the plastic crystal phase (dotted line) at 400 K and 70 000 bar. For clarity the function $f(\phi)$ of ice VIII has been shifted by 90 degrees to illustrate the similarity with that of ice VII.

Table 3 Helmholtz free energy for ices VIII, VII and for the plastic crystal phase. The Gibbs free energy was computed after adding pV to the Helmholtz free energy. The data marked with an asterisk correspond to calculations using the structure ice VII as obtained from the cooling of the plastic crystal. The density is given in g cm^{-3}

Phase	T/K	p/bar	ρ	A/N$k_B T$	G/N$k_B T$
Ice VIII	300	70 000	1.709	−9.36	20.23
Ice VII	300	70 000	1.707	−9.75	19.87
Ice VII*	300	70 000	1.707	−9.74	19.88
Plastic	400	70 000	1.638	−6.46	16.69
Water	300	1292	1.050	−15.45	−14.56

and Wang in which the dielectric constant of ice Ih was computed by switching off the charges of the molecules while having translational springs.[74] In Table 3 the free energies for the considered thermodynamic states are reported. Let us just mention, that the Pauling degeneracy entropy was added to the free energy of ice VII. This contribution was not added neither to ice VIII nor to the plastic crystal phase.

As it can be seen the Gibbs free energy of ice VII is smaller than that of ice VIII. Both phases have similar densities and internal energies and the higher stability of ice VII is mainly due to the contribution of the Pauling entropy (which is not present in ice VIII). Therefore for T = 300 K and p = 70 000 bar ice VII is more stable than ice VIII. By using thermodynamic integration the ice VII to ice VIII transition at 70 000 bar has been located at T = 69 K. In the same way the VII to plastic crystal transition has been located to occur at 377 K for a pressure of 70 000 bar. This value is consistent with the hysteresis loop found at 70 000 bar between the temperatures 350 and 390. Finally by using thermodynamic integration the fluid-plastic crystal transition was found to occur at a pressure of p = 62 000 bar for the 400 K isotherm. The fluid-plastic crystal transition was also determined by using direct coexistence simulations. An equilibrated configuration of the plastic crystal phase (432 molecules) was located on the left hand side of a simulation box, and put into contact with an equilibrated configuration of the fluid having 432 molecules. Molecules of the fluid phase overlapping with those of the solid phase at the fluid-plastic interface were deleted. Thus the total number of molecules in the direct coexistence simulations was of 858. We then performed MD simulations using Gromacs, while keeping the temperature at 400 K. Runs at different pressures were performed. At pressures below the melting point the solid phase will melt, whereas at pressures higher than the coexistence pressure the fluid phase will crystallise. The direct coexistence technique, was pioneered by Ladd and Woodcock,[75–77] and used recently by several authors.[78–89] In Fig. 7, the evolution of the density with time is shown for several pressures. As it can be seen for the low pressures (55 000 and 58 000 bar) the density decreases quickly indicating the melting of the plastic crystal. For high pressures (i.e. 65 000, 70 000 bar) the density of the system increases quickly indicating the freezing of the fluid into a plastic crystal phase. Thus the value of 62 000 bar obtained from free energy calculations is consistent with the results obtained from direct coexistence simulations.[84] Notice that in the direct coexistence simulations the melting of the plastic crystal, or the freezing of the water occurs in about 0.2 ns, which is about two orders of magnitude smaller than the time required to determine accurately the melting point of ice Ih at room pressure by direct
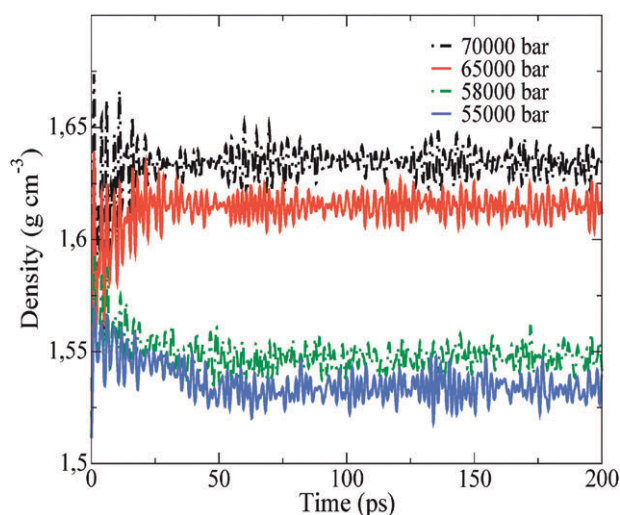
Fig. 7 Evolution of the density with time as obtained from direct coexistence MD simulations. All results were obtained for T = 400 K. Lines from the top to the bottom correspond to the pressures 70 000, 65 000, 58 000 and 55 000 bar, respectively.

coexistence simulations.[84] This is probably due to two different facts. First, the temperature is high (400 K instead of the temperature of about 250 K used in the ice Ih water direct interface simulations). Secondly the growth of the crystal is a somewhat more complex process for ice Ih since each water molecule must be located in a certain position and with a certain orientation to allow the ice Ih to grow. However, in the plastic crystal phase, the molecule must find the location, but the orientation is not so important since the molecules are rotating in the plastic crystal phase anyway.

Once an initial coexistence point has been found for the VIII–VII, VII-plastic and fluid-plastic crystal transitions, the rest of the coexistence lines will be obtained by Gibbs–Duhem simulations. In Fig. 8 these three coexistence lines are plotted. As it can be seen the fluid-plastic crystal and the VII-plastic crystal coexistence lines met at a triple point located around 352 K and 60 375 bar. This triple point can be used as initial coexistence point of the VII-fluid coexistence line. The fluid-VII coexistence line obtained from Gibbs–Duhem simulations has also been plotted in Fig. 8. At 300 K the Gibbs–Duhem integration predicts a fluid-VII coexistence pressure of about 51 000 bar, which is consistent with the coexistence pressure predicted from free energy calculations. The melting curve of ice VI intersects the melting curve of ice VII, generating a fluid-VI–VII triple point (the precise location is 301 K and 50 742 bar). This triple point can be used as initial point for the VI–VII coexistence curve. The VI–VII coexistence curve

This journal is © the Owner Societies 2009

Phys. Chem. Chem. Phys., 2009, **11**, 543–555 | 549
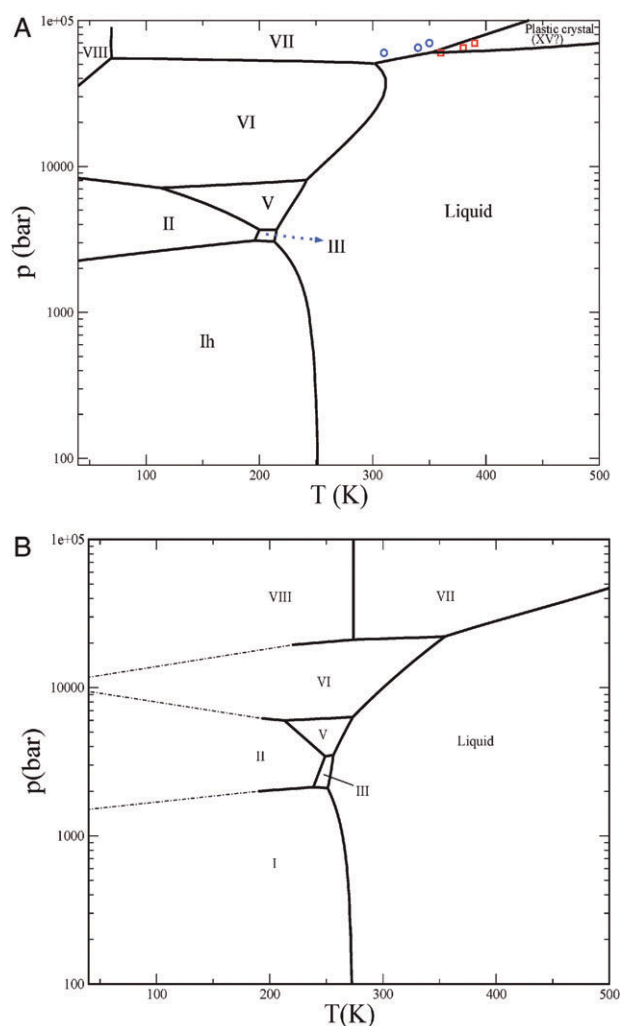
Fig. 8 (a) Global phase diagram for the TIP4P/2005 model. The squares correspond to the stability limit of ice VII when heated, whereas the circles correspond to the stability limit of the plastic crystal phase when cooled. (b) Experimental phase diagram of water.

intersects the VIII–VII coexistence curve at about 55 000 bar and 69 K. This generates an VI–VII–VIII triple point which can be used to initiate the VI–VIII coexistence line. The global phase diagram of the TIP4P/2005 (including the high pressure phases) is presented in Fig. 8. The experimental phase diagram is also presented in Fig. 8. The coexistence lines are given in tabular form in Tables 4–6. The triple points are given in Table 7.

As it can be seen the TIP4P/2005 reproduces qualitatively the phase diagram of water. Ice VIII is stable only at low temperatures. The coexistence line between ice VIII and ice VII is almost a vertical line. This is due to the fact that the densities of ices VII and VIII are practically identical for a certain temperature and pressure. There is a certain regime of temperatures where ice VII coexists with the liquid phase. There are three significant qualitative differences between the phase diagram of TIP4P/2005 and the experimental one. The first is that the VIII–VII transition temperature seems to be low as compared to experiment. It seems that models with a TIP4P geometry tend to underestimate the temperature of the order–disorder transitions (between ices having the same arrangement of oxygens but differing in the proton ordering). In fact we found in previous work[22] that also the XI-Ih transition was predicted to occur for the TIP4P model at a temperature lower than found experimentally. The second is the appearance of a plastic crystal phase for the TIP4P/2005 model. This plastic crystal phase has not been reported so far for real water. The third is the appearance of re-entrant melting in the melting curve of ice VI which is not found in the experimental phase diagram. The reason for the appearance of re-entrant melting in the melting curve of ices (from ice Ih up to ice VI) has been discussed previously.[20] The fluid–VI–VII triple point is located at 301 K and 50 742 bar, to be compared with the experimental value which is located at a temperature of 355 K and a pressure of about 22 000 bar. Thus, it seems that to bring the phase diagram of TIP4P/2005 into closer agreement with experiment the stability of ice VII should increase. In this way the fluid–VI–VII triple point would occur at lower pressures and the re-entrant portion of the melting curve of ice VI would occur in the metastable part of the melting curve. In Fig. 9 the equation of state of ices VIII and VII at 300 K are plotted as a function of pressure. For pressures below 35 000 bar ice VIII (as described by TIP4P/2005) is not mechanically stable and melts into a liquid phase. For pressures below 40 000 bar ice VII (as described by TIP4P/2005) is not mechanically stable and melts into a liquid phase. As it can be seen for a certain temperature and pressure ice VIII yields a slightly higher density than ice VII (the densities are quite similar anyway as also pointed out by Bartok and Baranyai[45]). As it can be seen the TIP4P/2005 model is not able to describe accurately the experimental values of the densities of ice VII. In fact it tends to underestimate the experimental values of the densities by about 5 per cent. This is striking since the TIP4P/2005 is

Table 4 Melting curve of the plastic crystal phase of the TIP4P/2005 as obtained from free energy calculations and Gibbs–Duhem integration (with isotropic NpT simulation performed for the fluid and for the cubic plastic crystal phase). The densities are given in g cm^{-3}. The residual internal energies are given in kcal mol^{-1}

T/K	p/bar	U_1	U_2	ρ_1	ρ_2
Fluid-plastic crystal					
340.00	60 193	−10.45	−10.03	1.574	1.622
360.00	60 486	−10.24	−9.85	1.572	1.613
380.00	61 135	−10.04	−9.73	1.565	1.610
400.00	62 000	−9.87	−9.58	1.562	1.609
420.00	63 108	−9.75	−9.43	1.565	1.607
440.00	64 390	−9.52	−9.30	1.564	1.608
460.00	66 042	−9.35	−9.12	1.560	1.607

Table 5 Melting curves of ices VI and VII for the TIP4P/2005 model as obtained from free energy calculations and Gibbs Duhem integration. The densities are given in g cm^{-3}. The internal energies in kcal mol^{-1} (only the residual part of the internal energy is reported)

T/K	p/bar	U_1	U_2	ρ_1	ρ_2
Fluid-VI					
244.97	8540	−12.23	−12.96	1.245	1.359
254.39	10 000	−12.02	−12.91	1.265	1.365
265.14	12 000	−11.98	−12.84	1.286	1.373
278.27	15 000	−11.77	−12.76	1.316	1.385
293.67	20 000	−11.55	−12.64	1.365	1.406
303.39	25 000	−11.38	−12.55	1.396	1.427
309.21	30 000	−11.26	−12.47	1.435	1.447
311.52	35 000	−11.21	−12.39	1.464	1.467
311.39	40 000	−11.15	−12.32	1.492	1.485
308.14	45 000	−11.03	−12.26	1.518	1.503
302.87	50 000	−10.98	−12.20	1.542	1.520
293.92	55 000	−10.97	−12.15	1.572	1.537
281.74	60 000	−10.89	−12.11	1.596	1.553
Fluid-VII					
352.00	60 375	−10.30	−10.46	1.578	1.663
340.00	58 066	−10.42	−10.57	1.570	1.658
320.00	54 276	−10.74	−10.74	1.565	1.651
300.00	50 988	−10.90	−10.90	1.549	1.646

Table 6 Solid–solid coexistence lines of the TIP4P/2005 model for the high pressure polymorphs (ice VII, VIII and plastic crystal) as obtained from free energy calculations and Gibbs–Duhem integration. The densities are given in g cm^{-3}. The internal energies in kcal mol^{-1} (only the residual part of the internal energy is reported)

T/K	p/bar	U_1	U_2	ρ_1	ρ_2
VII–plastic crystal					
440.00	101 354	−8.99	−8.49	1.749	1.728
420.00	90 168	−9.44	−8.81	1.729	1.698
400.00	80 146	−9.76	−9.19	1.707	1.674
390.00	75 596	−9.82	−9.33	1.693	1.659
377.00	70 000	−10.04	−9.53	1.681	1.645
360.00	63 292	−10.27	−9.79	1.666	1.623
350.00	59 665	−10.40	−9.95	1.656	1.617
VII–VIII					
69.70	55 000	−11.97	−12.01	1.719	1.718
69.00	70 000	−11.67	−11.71	1.758	1.758
69.49	80 000	−11.45	−11.48	1.781	1.782
VI–VII					
301.00	50 742	−12.19	−10.85	1.523	1.642
280.00	51 549	−12.29	−11.03	1.529	1.655
240.00	52 454	−12.50	−11.23	1.538	1.669
100.00	54 767	−13.15	−11.85	1.567	1.712
50.00	55 369	−13.38	−12.06	1.576	1.726
VI–VIII					
69.00	55 000	−12.14	−12.02	1.594	1.719
35.00	32 974	−12.90	−12.58	1.519	1.660

**Table 7** Triple points of the TIP4P/2005 model of water, between stable phases at high pressures

Phase boundary	T/K	p/bar
Fluid-VI–VII	301	50 742
Fluid-VII-plastic	352	60 375
VI–VII–VIII	69	55 000

able to describe the densities of ices Ih, II, III, IV, V, VI, IX and XII (for pressures up to 20 000 bar) within an error of about 1 per cent and for liquid water up to pressures of about 40 000 bar with an error of about 1 per cent. Thus it seems that there is something wrong in the model which prevents of describing accurately the densities of ices VIII and VII at high pressures. Notice that other water models as SPC, SPC/E and TIP4P do also underestimate significant the density of ice VII at high pressures. Further work is needed to understand the origin of that. One may suggest that the absence of polarisability, or the use of a non very accurate description of the repulsive part of the potential (by the LJ potential), or even the absence of LJ sites located on the hydrogen atoms (to introduce a further degree of anisotropy) may be responsible. The only model that reproduces the experimental densities of ice VII is TIP5P. This is shown in Table 8. However, this is not for free since this model overestimates by about 5–8 per cent[90] the densities of ices Ih, II, III, IV, V, VI, IX and XII. Thus TIP5P reproduces the densities of ice VII, but fails completely in describing the densities of the other polymorphs of water.[91–93]

Let us present the value of the dielectric constant of the plastic crystal phase. It should be pointed out that standard computer simulations (MD or standard MC) cannot be used to determine the dielectric constant of ices. Typical lengths of
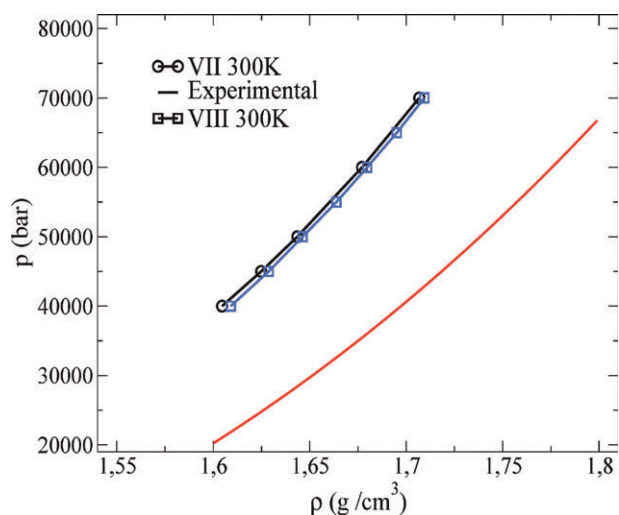
Fig. 9 Equation of state of ices VII (open circles) and VIII (open squares) for $T = 300$ K as obtained from computer simulation for the TIP4P/2005 model. The solid line on the right hand side correspond to the experimental results as given by Fei *et al.*[91]

the simulations (several ns or hundred of thousands of cycles) are not sufficient to sample the fluctuations of the polarisation of the solid. To compute dielectric constants of ices it is necessary either to introduce special moves within the Monte Carlo program, as those proposed by Rick and Haymet[94,95] or to use special techniques as that proposed recently by Lindberg and Wang.[74] Thus from our study we could not report the dielectric constant of ices VIII and VII. However we could compute the dielectric constant for the plastic crystal since the molecules are able to rotate rather quickly provoking important fluctuations of the total polarisation. We obtained a value of about 96(10) for the plastic crystal phase at 400 K and 70 000 bar. The dielectric constant of the plastic crystal phase (assuming it exists in real water) has not been reported. The experimental value[96] of the dielectric constant of ice VII at room temperature and for a pressure of 23 300 bar is of 105. Although it is difficult to compare dielectric constants obtained for somewhat different structures (ice VII and the plastic crystal phase are not the same solid), and somewhat different thermodynamic conditions, the comparison between both values appears as reasonable. For liquid water at room temperature and pressure the TIP4P/2005 predicts a dielectric

constant of about 60, whereas the experimental value is of 78. Thus the model underestimates the dielectric constant of liquid water by about 20 per cent. Also for ice Ih, TIP4P models seriously underestimate the dielectric constant.[74,94,95] Assuming that similar behaviour could be found for liquid water and the plastic ice, the prediction of the model for the plastic crystal phase seems to be lower than the experimental value of ice VII. The absence of polarisability is likely to be responsible for this deviation.

IV. Conclusions

In this work the high pressure region of the phase diagram of water has been determined by computer simulation by using the TIP4P/2005 model. By performing free energy calculations the relative stability of ices VIII and VII, and the melting curve of ice VII was obtained. When compressing water at 440 K, the freezing of water into a solid phase occurred in a few ns. The analysis of the solid allows to conclude that it is formed by a body center cubic lattice of oxygens, with the molecules rotating significantly. In summary a plastic crystal phase. It has also been found that ices VIII and VII transform into a plastic crystal phase at temperatures above 390 K and pressures below 70 000 bar. By performing free energy calculations the melting curve of the plastic crystal phase and the coexistence lines between the plastic crystal phase and ice VII could be determined. In this way a rather extensive region of the phase diagram for the TIP4P/2005 could be reported by the first time. The possible existence of other solid phases or even of other plastic crystal phases for the model should not be discarded yet. The TIP4P/2005 is able to describe qualitatively the phase diagram of water. The model (in common with the popular SPC/E and TIP4P models) fails to describe the density of ice VII along the room temperature isotherm, and underestimates with respect to experiment the stability of ice VII. This is in contrast with the excellent description provided for other coexistence lines and for the densities of other polymorphs appearing at pressures below 20 000 bar. Thus the model does not allow to describe quantitatively the behaviour of water at high pressures. Further work is needed to understand the origin of that. On the other hand the model predicts the existence of a new phase, a plastic crystal phase. Notice that all transitions found between the plastic crystal phase and

Table 8 Densities of ice VII as obtained from the NpT simulations of this work for the TIP4P/2005 and TIP5P models of water. The experimental data for ice VII are taken from ref. 91 and for the rest of polymorphs from ref. 92, except for ice II that was taken from ref. 93. Values of the densities of the other polymorphs were taken from ref. 27 for the TIP4P/2005 model and from ref. 90 for the TIP5P model

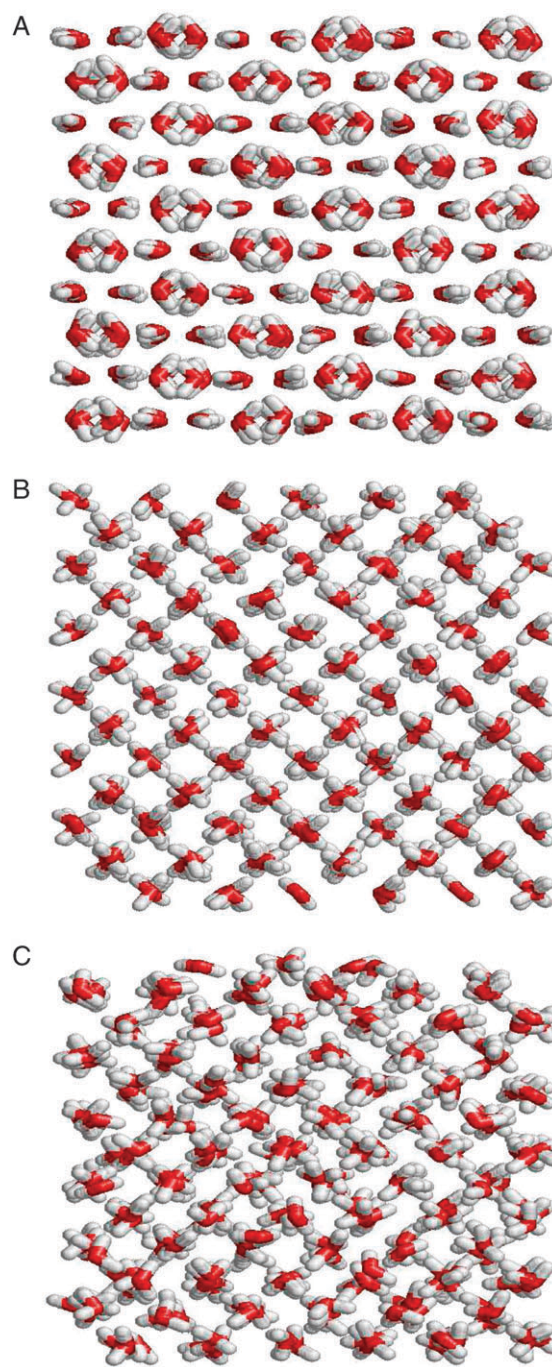| Phase	T/K	p/bar	ρ/g cm^{-3}		
			Expt	TIP4P/2005	TIP5P
VII	300	45 000	1.718	1.625	1.729
VII	300	70 000	1.810	1.707	1.814
I_h	250	0	0.920	0.921	0.976
II	123	0	1.190	1.199	1.284
III	250	2800	1.165	1.160	1.185
IV	110	0	1.272	1.293	1.371
V	223	5300	1.283	1.272	1.331
VI	225	11 000	1.373	1.380	1.447
IX	165	2800	1.194	1.190	1.231
XII	260	5	1.292	1.296	1.340

other phases (liquid or ice VII) were found to be first order, so that if the plastic crystal phase exists in real water there should be a first order phase transition separating it from ice VII. Interestingly Takii, Koga and Tanaka suggested[38] that the two set of melting curves reported experimentally at 100 000 bar could be due to the fact that these two groups were indeed measuring two different transitions, namely the ice VII to plastic crystal (that would correspond to the temperature of 600 K given by Mishima and Endo[97]) and the plastic crystal to liquid phase (that would correspond to the temperature of 687 K given by Datchi, Loubeyre and LeToullec[98]). Further experimental work is needed to clarify this point.

It would be of interest to study if such a plastic crystal phase does indeed exist for real water. If so it would correspond to ice XV (the precise Roman numeral may change if other solid phases of water are found experimentally before), and would probably be one of the few cases where computer simulation anticipates an experimental result. In case it exists it may dominate the melting curve of water at high temperatures. The nearly spherical shape of water makes possible the formation of a plastic crystal phase at high temperatures where the strength of the hydrogen bond in k_BT units is rather small and where the molecular shape (*i.e.* repulsive forces) play the leading role in the process of freezing. For hard dumbbells or spherocylinders the maximum anisotropy (as given by the ratio between the bond length and the width of the molecule) which allows the formation of a plastic crystal phase is of about 0.4.[99–104] Molecules with higher anisotropy freeze into an orientally ordered solid. Thus the formation of plastic crystal phases requires moderate anisotropy in the repulsive part of the potential (the importance of the attractive part decreases substantially at high temperatures). This seems to be the case of water, at least when described as a LJ center plus charges. Besides the experimental importance of a plastic crystal phase for water, its presence or absence should also have an impact on the community performing computer simulations of water. Its presence would indicate that current water models are able to predict qualitatively this new feature of the phase diagram of water. Its absence would also be significant since it would indicate that current water models are too spherical and they should be modified as to predict the disappearance of the plastic crystal phase.

Since a picture is worth a thousand words let us present an instantaneous snapshot of ices VII, VIII and of the plastic crystal. This is done in Fig. 10. The orientational disorder of the plastic crystal phase is shown clearly in the Figure.

Acknowledgements

Fig. 10 Snapshots of ices. (a) Snapshot of ice VIII at 300 K and 70 000 bar. (b) Snapshot of ice VII at 300 K and 70 000 bar. (c) Snapshot of the plastic crystal phase at 400 K and 70 000 bar.

References

1 G. Tammann, *Kristallisieren und Schmelzen*, Johann Ambrosius Barth, Leipzig, 1903.
2 G. Tammann, *Z. Phys. Chem.*, 1910, **68**, 205.
3 P. W. Bridgman, *Proc. Am. Acad. Sci. Arts*, 1912, **47**, 441.
4 P. W. Bridgman, *J. Chem. Phys.*, 1937, **3**, 597.
5 P. W. Bridgman, *J. Chem. Phys.*, 1937, **5**, 964.
6 C. Lobban, J. L. Finney and W. F. Kuhs, *Nature*, 1998, **391**, 268.
7 C. G. Salzmann, P. G. Radaelli, A. Hallbrucker, E. Mayer and J. L. Finney, *Science*, 2006, **311**, 1758.
8 P. H. Poole, F. Sciortino, U. Essmann and H. E. Stanley, *Nature*, 1992, **360**, 324.

9 O. Mishima and H. E. Stanley, *Nature*, 1998, **396**, 329.
10 P. G. Debenedetti, *J. Phys.: Condens. Matter*, 2003, **15**, R1669.
11 C. Lobban, J. L. Finney and W. F. Kuhs, *J. Chem. Phys.*, 2000, **112**, 7169.
12 P. Ball, *Life's Matrix. A Biography of Water*, University of California Press, Berkeley, 2001.
13 F. Franks, *Water a Matrix of Life*, Royal Society of Chemistry, Cambridge, 2000.
14 J. L. Finney, *Philos. Trans. R. Soc. London, Ser. B*, 2004, **359**, 1145.
15 J. A. Barker and R. O. Watts, *Chem. Phys. Lett.*, 1969, **3**, 144.
16 A. Rahman and F. H. Stillinger, *J. Chem. Phys.*, 1971, **55**, 3336.
17 M. D. Morse and S. A. Rice, *J. Chem. Phys.*, 1982, **76**, 650.
18 H. J. C. Berendsen, J. R. Grigera and T. P. Straatsma, *J. Phys. Chem.*, 1987, **91**, 6269.
19 W. L. Jorgensen, J. Chandrasekhar, J. D. Madura, R. W. Impey and M. L. Klein, *J. Chem. Phys.*, 1983, **79**, 926.
20 E. Sanz, C. Vega, J. L. F. Abascal and L. G. MacDowell, *Phys. Rev. Lett.*, 2004, **92**, 255701.
21 C. Vega, E. Sanz and J. L. F. Abascal, *J. Chem. Phys.*, 2005, **122**, 114507.
22 C. Vega, J. L. F. Abascal, E. Sanz, L. G. MacDowell and C. McBride, *J. Phys.: Condens. Matter*, 2005, **17**, S3283.
23 C. McBride, C. Vega, E. Sanz, L. G. MacDowell and J. L. F. Abascal, *Mol. Phys.*, 2005, **103**, 1.
24 J. L. F. Abascal and C. Vega, *J. Chem. Phys.*, 2005, **123**, 234505.
25 J. L. F. Abascal, E. Sanz, R. G. Fernández and C. Vega, *J. Chem. Phys.*, 2005, **122**, 234511.
26 J. L. Aragones, E. G. Noya, J. L. F. Abascal and C. Vega, *J. Chem. Phys.*, 2007, **127**, 154518.
27 E. G. Noya, C. Menduina, J. L. Aragonés and C. Vega, *J. Phys. Chem. C*, 2007, **111**, 15877.
28 M. Martin-Conde, L. G. MacDowell and C. Vega, *J. Chem. Phys.*, 2006, **125**, 116101.
29 C. Vega, J. L. F. Abascal and I. Nezbeda, *J. Chem. Phys.*, 2006, **125**, 034503.
30 C. Vega and E. de Miguel, *J. Chem. Phys.*, 2007, **126**, 154707.
31 I. Svishchev and P. G. Kusalik, *Phys. Rev. Lett.*, 1994, **73**, 975.
32 M. Matsumoto, S. Saito and I. Ohmine, *Nature*, 2002, **416**, 409.
33 L. Vrbka and P. Jungwirth, *J. Phys. Chem. B*, 2006, **110**, 18126.
34 D. Quigley and P. M. Rodger, *J. Chem. Phys.*, 2008, **128**, 154518.
35 A. Laio and M. Parrinello, *Proc. Natl. Acad. Sci. U. S. A.*, 2002, **99**, 12562.
36 D. H. Dolan, J. N. Johnson and Y. M. Gupta, *J. Chem. Phys.*, 2005, **123**, 64702.
37 D. H. Dolan, M. D. Knudson, C. A. Hall and C. Deeney, *Nat. Phys.*, 2007, **3**, 339.
38 Y. Takii, K. Koga and H. Tanaka, *J. Chem. Phys.*, 2008, **128**, 204501.
39 R. Hemley, A. P. Jephcoat, H. K. Mao, C. S. Zha, L. W. Finger and D. E. Cox, *Nature*, 1987, **330**, 737.
40 M. Somayazulu, J. Shu, C. Zha, A. F. Goncharov, O. Tschauner, H. Mao and R. Hemley, *J. Chem. Phys.*, 2008, **128**, 64510.
41 J. L. F. Abascal, R. G. Fernandez, L. G. MacDowell, E. Sanz and C. Vega, *J. Mol. Liq.*, 2007, **136**, 214.
42 J. Kolafa, F. Moucka and I. Nezbeda, *Collect. Czech. Chem. Commun.*, 2008, **73**, 481.
43 P. Dyer, H. Docherty and P. Cummings, *J. Chem. Phys.*, 2008, **129**, 024508.
44 A. Ghoufi, F. Goujon, V. Lachet and P. Malfreyt, *J. Chem. Phys.*, 2008, **128**, 154716.
45 A. Bartok and A. Baranyai, *J. Cryst. Solids*, 2007, **353**, 2698.
46 C. Vega, J. L. F. Abascal, M. M. Conde and J. L. Aragones, *Faraday Discuss.*, 2009, **141**, DOI: 10.1039/b805531a.
47 V. F. Petrenko and R. W. Whitworth, *Physics of Ice*, Oxford University Press, Oxford, 1999.
48 D. Eisenberg and W. Kauzmann, *The Structure and Properties of Water*, Oxford University Press, London, 1969.
49 W. F. Kuhs, J. L. Finney, C. Vettier and D. V. Bliss, *J. Chem. Phys.*, 1984, **81**, 3612.
50 B. Kamb and B. L. Davis, *Proc. Natl. Acad. Sci. U. S. A.*, 1964, **52**, 1433.
51 G. P. Johari, A. Lavergne and E. Whalley, *J. Chem. Phys.*, 1974, **61**, 4292.
52 J. D. Bernal and R. H. Fowler, *J. Chem. Phys.*, 1933, **1**, 515.
53 L. Pauling, *J. Am. Chem. Soc.*, 1935, **57**, 2680.
54 V. Buch, P. Sandler and J. Sadlej, *J. Phys. Chem. B*, 1998, **102**, 8641.
55 M. P. Allen and D. J. Tildesley, *Computer Simulation of Liquids*, Oxford University Press, 1987.
56 D. van der Spoel, P. J. van Maaren and H. J. C. Berendsen, *J. Chem. Phys.*, 1998, **108**, 10220.
57 M. Lísal, J. Kolafa and I. Nezbeda, *J. Chem. Phys.*, 2002, **117**, 8892.
58 S. W. Rick, *J. Chem. Phys.*, 2004, **120**, 6085.
59 D. Frenkel and B. Smit, *Understanding Molecular Simulation*, Academic Press, London, 2002.
60 M. Parrinello and A. Rahman, *J. Appl. Phys.*, 1981, **52**, 7182.
61 S. Yashonath and C. N. R. Rao, *Mol. Phys.*, 1985, **54**, 245.
62 J. K. Johnson, J. A. Zollweg and K. E. Gubbins, *Mol. Phys.*, 1993, **78**, 591.
63 D. Frenkel and A. J. C. Ladd, *J. Chem. Phys.*, 1984, **81**, 3188.
64 C. Vega and E. G. Noya, *J. Chem. Phys.*, 2007, **127**, 154113.
65 C. Vega, E. Sanz, E. G. Noya and J. L. F. Abascal, *J. Phys.: Condens. Matter*, 2008, **20**, 153101.
66 D. A. Kofke, *J. Chem. Phys.*, 1993, **98**, 4149.
67 D. A. Kofke, in *Monte Carlo Methods in Chemical Physics*, ed. D. M. Ferguson, J. I. Siepmann and D. G. Truhlar, John Wiley and Sons, 1998, vol. 105, p. 405.
68 D. V. der Spoel, E. Lindahl, B. Hess, G. Groenhof, A. E. Mark and H. J. C. Berendsen, *J. Comput. Chem.*, 2005, **26**, 1701.
69 S. Nosé, *Mol. Phys.*, 1984, **52**, 255.
70 W. G. Hoover, *Phys. Rev. A*, 1985, **31**.
71 M. Parrinello and A. Rahman, *J. Appl. Phys.*, 1981, **52**, 7182.
72 S. Nosé and M. L. Klein, *Mol. Phys.*, 1983, **50**, 1055.
73 U. Essmann, L. Perera, M. L. Berkowitz, T. Darden, H. Lee and L. G. Pedersen, *J. Chem. Phys.*, 1995, **103**, 8577.
74 G. E. Lindberg and F. Wang, *J. Phys. Chem. B*, 2008, **112**, 6436.
75 A. J. C. Ladd and L. Woodcock, *Chem. Phys. Lett.*, 1977, **51**, 155.
76 A. J. C. Ladd and L. Woodcock, *Mol. Phys.*, 1978, **36**, 611.
77 J. Cape and L. Woodcock, *Chem. Phys. Lett.*, 1977, **59**, 271.
78 J. Q. Broughton and G. H. Gilmer, *J. Chem. Phys.*, 1986, **84**, 5749.
79 R. L. Davidchack and B. B. Laird, *J. Chem. Phys.*, 1998, **108**, 9452.
80 J. R. Morris and X. Song, *J. Chem. Phys.*, 2002, **116**, 9352.
81 P. M. Agrawal, B. M. Rice and D. L. Thompson, *J. Chem. Phys.*, 2003, **119**, 9617.
82 O. A. Karim and A. D. J. Haymet, *J. Chem. Phys.*, 1988, **89**, 6889.
83 T. Bryk and A. D. J. Haymet, *J. Chem. Phys.*, 2002, **117**, 10258.
84 R. G. Fernandez, J. L. F. Abascal and C. Vega, *J. Chem. Phys.*, 2006, **124**, 144506.
85 J. L. F. Abascal, R. G. Fernandez, C. Vega and M. A. Carignano, *J. Chem. Phys.*, 2006, **125**, 166101.
86 T. J. Frankcombe and G. J. Kroes, *J. Phys. Chem. C*, 2007, **111**, 13044.
87 J. Wang, S. Yoo, J. Bai, J. R. Morris and X. C. Zeng, *J. Chem. Phys.*, 2005, **123**, 036101.
88 J. Vatamanu and P. G. Kusalik, *J. Phys. Chem. B*, 2006, **110**, 15896.
89 E. G. Noya, C. Vega and E. de Miguel, *J. Chem. Phys.*, 2008, **128**, 154507.
90 C. Vega, C. McBride, E. Sanz and J. L. Abascal, *Phys. Chem. Chem. Phys.*, 2005, **7**, 1450.
91 Y. Fei, H.-K. Mao and R. J. Hemley, *J. Chem. Phys.*, 1993, **99**, 5369.
92 V. F. Petrenko and R. W. Whitworth, *Physics of Ice*, Oxford University Press, 1999.
93 A. D. Fortes, I. G. Wood, M. Alfredsson, L. Vočadlo and K. S. Knight, *J. Appl. Crystallogr.*, 2005, **38**, 612.
94 S. W. Rick and A. D. J. Haymet, *J. Chem. Phys.*, 2003, **118**, 9291.
95 S. W. Rick, *J. Chem. Phys.*, 2005, **122**, 094504.
96 G. P. Johari, A. Lavergne and E. Whalley, *J. Chem. Phys.*, 1974, **61**, 4292.
97 O. Mishima and S. Endo, *J. Chem. Phys.*, 1978, **68**, 4417.
98 F. Datchi, F. P. Loubeyre and R. LeToullec, *Phys. Rev. B: Condens. Matter Mater. Phys.*, 2000, **61**, 6535.

99 C. Vega, E. P. A. Paras and P. A. Monson, *J. Chem. Phys.*, 1992, **96**, 9060.

100 C. Vega, E. P. A. Paras and P. A. Monson, *J. Chem. Phys.*, 1992, **97**, 8543.

101 E. P. A. Paras, C. Vega and P. A. Monson, *Mol. Phys.*, 1992, **77**, 803.

102 C. Vega and P. A. Monson, *J. Chem. Phys.*, 1997, **107**, 2696.

103 P. Bolhuis and D. Frenkel, *J. Chem. Phys.*, 1997, **106**, 666.

104 P. A. Monson and D. A. Kofke, in *Advances in Chemical Physics*, ed. I. Prigogine and S. A. Rice, John Wiley and Sons, 2000, vol. 115, p. 113.

This journal is © the Owner Societies 2009

Phys. Chem. Chem. Phys., 2009, **11**, 543–555 | 555